Kinetic and Physiological Effects of Alterations in Homologous Isocitrate-Binding Sites of Yeast NAD$^+$-Specific Isocitrate Dehydrogenase†

An-Ping Lin, Mark T. McCammon, and Lee McAlister-Henn*

Department of Biochemistry, University of Texas Health Science Center, San Antonio, Texas 78229-3900

Received June 6, 2001; Revised Manuscript Received August 21, 2001

ABSTRACT: Yeast NAD$^+$-specific isocitrate dehydrogenase is an allosterically regulated octameric enzyme composed of four each of two homologous but nonidentical subunits designated IDH1 and IDH2. Models based on the crystallographic structure of *Escherichia coli* isocitrate dehydrogenase suggest that both yeast subunits contain isocitrate-binding sites. Identities in nine residue positions are predicted for the IDH2 site whereas four of the nine positions differ between the IDH1 and bacterial enzyme sites. Thus, we speculate that the IDH2 site is catalytic and that the IDH1 site may bind but not catalytically alter isocitrate. This was examined by kinetic analyses of enzymes with independent and concerted replacement of residues in each yeast IDH subunit site with the residues that differ in the other subunit site. Mutant enzymes were expressed in a yeast strain containing disrupted *IDH1* and *IDH2* loci and affinity-purified for kinetic analyses. The primary effects of various residue replacements in IDH2 were reductions of 30−>300-fold in V_{max} values, consistent with the catalytic function of this subunit. In contrast, replacement of all four residues in IDH1 produced a 17-fold reduction in V_{max} under the same assay conditions, suggesting that the IDH1 site is not the primary catalytic site. However, single or multiple residue replacements in IDH1 uniformly increased half-saturation concentrations for isocitrate, implying that isocitrate can be bound at this site. Both subunits appear to contribute to cooperativity with respect to isocitrate, but AMP activation is lost only with residue replacements in IDH1. Overall, results are consistent with isocitrate binding by IDH2 for catalysis and with isocitrate binding by IDH1 being a prerequisite for allosteric activation by AMP. The effects of residue substitutions on enzyme function in vivo were assessed by analysis of various growth phenotypes. Results indicate a positive correlation between the level of IDH catalytic activity and the ability of cells to grow with acetate or glycerol as carbon sources. In addition, lower levels of activity are associated with increased production of respiratory-deficient (petite) segregants.

The oxidative decarboxylation of isocitrate to form α-ketoglutarate is a highly regulated reaction of the tricarboxylic acid cycle. Yeast and mammalian mitochondrial NAD$^+$-specific isocitrate dehydrogenases are structurally complex and subject to multiple allosteric regulatory controls. In particular, sensitive response to the positive allosteric regulator ADP in mammalian cells (*1*) or AMP in yeast is the basis for the hypothesis that rates of respiration are finely controlled by cellular energy charge [i.e., the relative concentrations of adenine nucleotides (*2*)]. In contrast, the same reaction in *Escherichia coli* is catalyzed by a homodimeric NADP$^+$-specific enzyme (subunit molecular weight = 45764) that is regulated by phosphorylation rather than by allostery (*3*, *4*). The target for phosphorylation/inactivation of *E. coli* isocitrate dehydrogenase is a single residue, Ser-113, in the isocitrate-binding site. Phosphorylation or an S113D replacement essentially eliminates binding of isocitrate (*5*). In vivo, this modification redirects flux of isocitrate from the tricarboxylic acid cycle into the glyoxylate pathway for two-carbon assimilation (*6*).

In addition to allosteric control of flux, yeast IDH[1] has been identified as a mitochondrial mRNA binding protein (*7*). This IDH/mRNA interaction appears to negatively regulate translation of the transcripts (*8*) that encode subunits of electron transport complexes. The mRNAs also inhibit IDH activity (*9*), suggesting a novel mechanism for reciprocal control of flux through the tricarboxylic acid cycle and respiratory complex biogenesis.

The NAD$^+$-specific IDH of *Saccharomyces cerevisiae* is an octamer composed of two subunits in an α_4:β_4 ratio (*10*). The two subunits, designated IDH1 and IDH2 (respective molecular weights of 38001 and 37755), are encoded by distinct nuclear genes and share 42% primary sequence identity (*11*, *12*). Gene disruption analyses have shown that both subunits are essential for cellular activity and that yeast strains containing disruptions of *IDH1* and/or *IDH2* genes fail to grow on acetate as a carbon source (*11*), a phenotype shared with yeast mutants lacking other tricarboxylic acid cycle enzymes including malate dehydrogenase (*13*) and citrate synthase (*14*).

Despite differences in cofactor specificity and holoenzyme structure, the IDH1 and IDH2 subunits of the yeast enzyme each share ∼32% residue sequence identity with the *E. coli* enzyme. Because of this similarity, the well-defined three-dimensional structure of the bacterial enzyme (*15*−*17*) has served as a very useful model for structural/functional analyses of the yeast enzyme. For example, as illustrated in Figures 1 and 2, sequence alignments suggest that both IDH1 and IDH2 contain isocitrate-binding sites. The putative binding site in IDH2 contains residues identical to those comprising the isocitrate/Mg^{2+} site of the bacterial enzyme

† Supported by NIH Grant GM51265.

* To whom correspondence should be addressed. Phone: (210) 567-3782. Fax: (210) 567-6595. E-mail: henn@uthscsa.edu.

[1] Abbreviations: IDH, NAD$^+$-specific isocitrate dehydrogenase; SDS, sodium dodecyl sulfate; HPLC, high-performance liquid chromatography.

10.1021/bi0111707 CCC: $20.00
Published on Web 10/30/2001

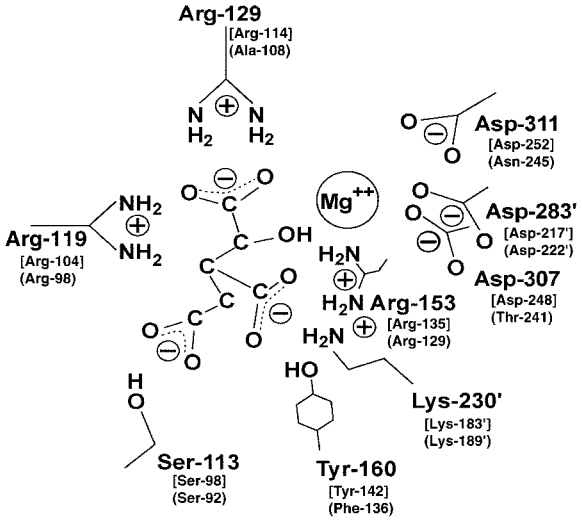

FIGURE 1: Model of isocitrate-binding sites. The diagram of residues in the isocitrate/Mg^{2+} binding site of *E. coli* isocitrate dehydrogenase is based on a representation by Hurley et al. (*17*) from the X-ray crystallographic structure of the enzyme. Identities of residues in the putative yeast IDH2 isocitrate/Mg^{2+} and IDH1 isocitrate-binding sites (shown in brackets and parentheses, respectively) are based on amino acid sequence alignments (Figure 2) and on structural modeling (*39*, *40*) of these sequences with the *E. coli* structure (data not shown). The residues indicated by prime symbols are from the other subunit of the functional dimer.

(*17*), suggesting that this is the catalytic site of the yeast enzyme. The putative binding site in IDH1, however, contains identities for only five of nine residues in the bacterial site, suggesting that IDH1 may bind isocitrate but is unlikely to catalyze its decarboxylation. We initially tested this idea by mutagenesis of residues homologous to bacterial Ser-113 (*18*). An S98A replacement in IDH2 was found to produce a significant reduction in V_{max} with little effect on allosteric properties, whereas an S92A replacement in IDH1 had little effect on V_{max} but significantly reduced cooperativity with respect to isocitrate as well as allosteric activation by AMP. These data supported the idea of regulatory function for IDH1 and catalytic function for IDH2.

Additional evidence for differential function of the yeast IDH subunits was derived from mutagenesis of putative adenine nucleotide binding sites, again based on the bacterial enzyme structure (*19*). Replacement in IDH2 of two adjacent residues (Asp-286 and Ile-287) corresponding to key discriminatory residues for NAD^+/$NADP^+$ binding in bacterial enzymes (*20*) again had a primary effect on V_{max} due to a significant increase in the K_m for NAD^+. In contrast, replacement in IDH1 of the corresponding residues (Asp-279 and Ile-280) produced a primary defect in AMP activation. These results also suggested that the catalytic isocitrate/Mg^{2+}/NAD^+ binding sites in the yeast enzyme are primarily contained in IDH2 and regulatory isocitrate/AMP-binding sites are primarily contained in IDH1.

We also have evidence for a model in which the basic intrinsic structural/functional unit of the octameric yeast enzyme is a heterodimer of the two subunits (*19*, *21*). Yeast two-hybrid assays indicated extensive interaction between IDH1 and IDH2 but no interaction between like subunits (IDH1 with IDH1 or IDH2 with IDH2). Also, each subunit can be affinity-purified with the histidine-tagged form of the other subunit but not with the histidine-tagged form of the identical subunit. An important extension of this model is based on the structure of the *E. coli* enzyme that showed, whereas each subunit in the bacterial homodimer contains an active site, at least two residues (designated by prime symbols in Figure 1) in each active site are contributed by the other subunit. We used mutagenesis to test the possibility of similar contributions by distinct subunits in the yeast enzyme. Results indicated that residues designated by prime symbols in Figure 1 in each of the IDH1 and IDH2 isocitrate-binding sites are contributed by the other subunit (IDH2 and IDH1, respectively) in the heterodimer (*21*). These reciprocal contributions suggest a potential mechanism for communication between the active sites of IDH1 and IDH2.

Thus, our current hypothesis is that the highly homologous polypeptides of the yeast enzyme have evolved simultaneously to optimize binding by IDH1 of regulatory ligands (isocitrate and AMP) that are chemically similar to the substrate (isocitrate/Mg^{2+}) and cofactor (NAD^+) bound by IDH2. This study focuses on the presumed catalytic IDH2 and cooperative IDH1 isocitrate-binding sites of the yeast enzyme as a model for this evolution of differential function. Reasoning that the four residue differences between the subunit active sites (Figure 1) could indicate permissive alternatives for isocitrate binding, we analyzed mutant enzymes containing residues in each subunit corresponding to those in similar positions in the other subunit (Figure 2). Our kinetic analyses elucidate some subunit-specific functions of these residues and potential mechanisms for communication between catalytic and regulatory sites. Also, by assessing a number of growth phenotypes of yeast transformants, we examined the metabolic consequences of expression of these mutant forms of a tricarboxylic acid cycle enzyme.

EXPERIMENTAL PROCEDURES

Yeast Strains and Growth Conditions. Wild-type and mutant forms of isocitrate dehydrogenase were expressed in a haploid yeast strain, IDHΔ12L (*MATα ade2-1 can1-100 his3-11,15 leu2-3,112 trp1-1 ura3-1* Δ*idh1::LEU2* Δ*idh2::HIS3*), containing deletion/disruption mutations in *IDH1* and *IDH2* loci (*22*). Transformants of this strain were maintained on agar plates containing minimal YNB medium (0.17% yeast nitrogen base, 0.5% ammonium sulfate, pH 6.5) with 2% glucose and nutrients as needed to supplement auxotrophic requirements and to select for maintenance of plasmids.

Growth phenotype analyses were conducted using Ura^+ transformants of IDHΔ12L harboring plasmids for expression of IDH1 and IDH2 (see below). Growth with various carbon sources was evaluated by streaking transformant strains onto YP plates (1% yeast extract, 2% Bacto-peptone) containing 20 mg/L adenine hemisulfate and, as carbon source, either 2% glucose, ethanol, or acetate. Colony sizes were compared after 2−5 days of incubation at 30 °C. Culture growth rates in YP medium containing 3% glycerol were monitored every 2 h over a 36 h period by measuring optical density at 600 nm. Doubling times were calculated as the average of values from two independent experiments. Petite frequencies were determined using the *ade2* locus that permits identification of respiratory-sufficient and respiratory-deficient (petite) segregants as large red and small white colonies, respectively.

FIGURE 2: Amino acid sequence alignments of yeast IDH1 and IDH2 with *E. coli* isocitrate dehydrogenase. Identical residues in aligned sequences are indicated by bold type, and gaps introduced to maximize identity are indicated by dashes. Bacterial residues in the catalytic isocitrate-binding site are identified; yeast residues in homologous positions are underlined. Residue replacements in this study are indicated above the sequences.

For these assays, transformants were cultured overnight in SC medium (YNB medium containing complete supplements except uracil, Sigma) with glucose, and dilutions of the cultures were plated onto YP glucose plates. Red and white colonies were scored after 3 days of incubation at 30 °C. Each transformant was independently assayed at least three times.

Expression and Purification of Mutant Enzymes. Oligonucleotide-directed mutagenesis was performed and described by Panisko (*23*) to introduce codon changes for residues in IDH1 (A108R, F136Y, or T241D plus N245D) or in IDH2 (R114A, Y142F, or D248T plus D252N). Sequenced DNA fragments containing mutations in the *IDH1* or *IDH2* genes were subcloned into p*IDH1/IDH2*^{His} or into p*IDH1*^{His}*/IDH2*, respectively, as described (*23*). These plasmids, which are derivatives of pRS316 (a centromere-based *URA3* plasmid, *24*), contain both *IDH* genes with pentahistidine codons at the 3′ end of the coding region for one subunit and provide normal mitochondrial levels of IDH (*19*). Subsequent subcloning and additional mutagenesis steps were used to combine mutations within each subunit gene (*23*), producing plasmids designated p*IDH1*^{A108R,F136Y,T241D,N245D}*/IDH2*^{His} and p*IDH1*^{His}*/IDH2*^{R114A,Y142F,D248T,D252N}.

For analysis of cellular expression, protein extracts were prepared by glass bead lysis of harvested yeast cells as previously described (*13*). Protein concentrations were determined by the Bradford dye binding assay (*25*) using bovine serum albumin as the standard. Samples with equivalent cellular protein concentrations were electrophoresed on 10% polyacrylamide/sodium dodecyl sulfate gels and transferred to polyvinylidine difluoride membranes. Immunochemical analysis was based on an antiserum for yeast NAD^+−isocitrate dehydrogenase (*10*) and detection by the enhanced chemiluminescence method.

For purification of histidine-tagged enzymes, precultures were grown for 16 h in YNB medium containing 2% glucose under conditions for plasmid selection. The precultures were diluted into 1−2 L of rich YP medium containing 2% ethanol to increase levels of isocitrate dehydrogenase expression (*26*), and cells were harvested at A_{600nm} = 1.0−1.5. Affinity purification was conducted using Ni^{2+}-NTA resin (Qiagen) as previously described (*19*). Concentrations of purified proteins were determined by measuring absorbance at 280 nm and using a molar extinction coefficient of 168820 M^{-1} cm^{-1} estimated by the method of Pace et al. (*27*). Purity and subunit composition were examined by electrophoresis of samples of each purified enzyme on 10% polyacrylamide/SDS gels and staining with Coomassie Blue. The purified wild-type enzyme and mutant enzymes containing four residue changes were also examined by size exclusion HPLC, using a Superdex 200 H/R 10/30 column (Amersham-Pharmacia) and size standards ranging in molecular weight from 20000 to 437000. The buffer used for chromatography contained 10 mM Tris-HCl (pH 7.4), 50 mM NaCl, 3 mM $MgCl_2$, and 5% glycerol.

Kinetic Analyses. Isocitrate dehydrogenase activity was measured using assays containing 40 mM Tris-HCl, pH 7.4, and 4 mM $MgCl_2$ (*19*, *21*). Preliminary kinetic analyses were conducted with 0.25 mM NAD^+ (*23*). However, we found it necessary to use at least 0.5 mM NAD^+ at saturating

concentrations of isocitrate to obtain similar V_{max} values for wild-type enzymes in the presence or absence of AMP. Kinetic parameters for mutant enzymes were initially determined with 0.5 mM NAD^+ for comparison with wild-type parameters. For measurement of $S_{0.5}$ values for isocitrate, D-isocitrate concentrations ranged from 0 to as high as 15 mM for some mutant enzymes (D-isocitrate concentrations were calculated as 50% of the total DL-isocitrate). For measurement of $S_{0.5}$ values for NAD^+, the isocitrate concentration was set at five times the measured $S_{0.5}$ value for isocitrate for each enzyme, and NAD^+ concentrations ranged from 0 to 3.0 mM. For mutant enzymes that exhibited increased $S_{0.5}$ values for NAD^+ relative to wild-type enzymes, isocitrate saturation curves were repeated at higher concentrations of NAD^+ as described in the text. Also, for some mutant enzymes, $S_{0.5}$ values for isocitrate were measured with $MgCl_2$ concentrations ranging from 4.0 to 14 mM. Assays were initiated by addition of enzyme (~1.0 μg of wild-type enzyme and as much as 10 μg of some mutant enzymes per 1.0 mL assay). A unit of activity is defined as production of 1 μmol of NADH/min at 24 °C. V_{max} values are the maximal rates per milligram of purified IDH and, with $S_{0.5}$ values, were obtained by Hanes plot analyses of initial velocity data (*28*).

RESULTS

Construction and Expression of Mutant Enzymes. Our structural models for yeast IDH1 and IDH2 isocitrate-binding sites are based on the catalytic site of *E. coli* isocitrate dehydrogenase as illustrated in Figure 1. Of the nine residues shown in the bacterial site, two (Asp-283′ and Lys-230′) are contributed by the other subunit of the homodimer. Similarly, we have evidence that the "IDH2 active site" includes two residues from IDH1 (Asp-217′ and Lys-183′) and that the "IDH1 active site" includes two residues from IDH2 [Asp-222′ and Lys-189′ (*21*)]. All nine bacterial residues in the isocitrate/Mg^{2+} binding site are conserved in the putative IDH2 site, but there are four residue differences in the projected IDH1 site. Ala-108 in IDH1 is present in the position occupied by Arg-129 of the bacterial enzyme. The latter residue is one in a cluster of arginines that form hydrogen bonds with isocitrate (*17*). The IDH1 site also lacks two residues that bind or facilitate binding of Mg^{2+} (IDH1 Thr-241/Asn-245 versus bacterial Asp-307/Asp-311). Finally, the IDH1 site contains Phe-136 at a position occupied by bacterial Tyr-160, a residue important for the dehydrogenation step in catalysis (*29*). On the basis of these differences and previous mutagenesis of the yeast enzyme (*18*, *19*), we suggest that the IDH1 site binds but does not chemically modify isocitrate and is unlikely to bind Mg^{2+}. Thus, while the IDH2 site is believed to be catalytic, binding of isocitrate by IDH1 is believed to be important for cooperative characteristics of the enzyme.

To test these functional assignments for each subunit, each of the four nonconserved residues of IDH1 were replaced with the corresponding residues from IDH2 [and the *E. coli* enzyme, Figure 2 (*23*)]. Reciprocal replacements, rather than neutral alanine substitutions, were chosen because of specific interest in determining whether substitution of residues involved in catalytic binding of isocitrate would be permissive for cooperative binding of isocitrate. Conversely, to test their catalytic roles, the analogous residues of IDH2 were replaced with the four corresponding residues of IDH1 [Figure 2 (*23*)]. Individual residue replacements were made initially with the exception that, because of their proximity and presumed equivalence of function, simultaneous changes were made for Thr-241 and Asn-245 in IDH1 and for Asp-248 and Asp-252 in IDH2. Mutant alleles for each subunit were contained in plasmids carrying a histidine-tagged allele of the other subunit (*19*). Thus, plasmids constructed to test IDH1 function contained (with $IDH2^{His}$) *IDH1*, $IDH1^{A108R}$, $IDH1^{F136Y}$, or $IDH1^{T241D,N245D}$. Plasmids constructed to test IDH2 function contained (with $IDH1^{His}$) *IDH2*, $IDH2^{R114A}$, $IDH2^{Y142A}$, or $IDH2^{D248T,D252N}$ (*23*). Subsequently, subcloning was used to construct plasmids containing all four codon changes in the gene for each subunit ($IDH1^{A108R,F136Y,T241D,N245D}$/$IDH2^{His}$ and $IDH1^{His}$/$IDH2^{R114A,Y142F,D248T,D252N}$, *23*).

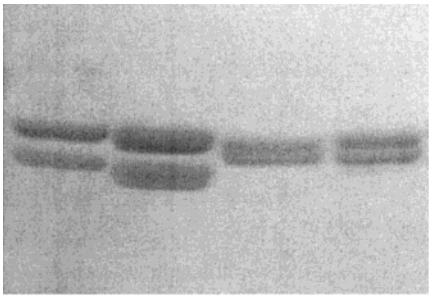

FIGURE 3: Electrophoretic analysis of affinity-purified wild-type and mutant enzymes. Histidine-tagged forms of IDH were expressed and purified as described in Experimental Procedures. Samples used for electrophoresis and Coomassie Blue staining were 10−15 μg of $IDH1^{His}$/IDH2 (lane 1), $IDH1^{His}$/$IDH2^{R114A,Y142F,D248T,D252N}$ (lane 2), IDH1/$IDH2^{His}$ (lane 3), and $IDH1^{A108R,F136Y,T241D,N245D}$/$IDH2^{His}$ (lane 4). In each lane, the slower migrating band is IDH1 and the faster migrating band is IDH2.

Plasmids were transformed into a host yeast strain containing disruptions in chromosomal *IDH1* and *IDH2* loci (*22*). Wild-type and mutant forms of IDH were purified from cell extracts by Ni^{2+}-NTA affinity chromatography as described in Experimental Procedures. Approximately equivalent amounts of enzymes (0.8−1.0 mg) were obtained per liter of harvested cells with this purification scheme. Thus, the mutant enzymes are stably expressed and can be purified with yields similar to those of the wild-type affinity-tagged enzymes. As illustrated in Figure 3, approximately equimolar amounts of both subunits are present in the purified wild-type and mutant enzymes containing four residue changes. These wild-type and mutant enzymes also exhibit similar elution patterns following size exclusion chromatography as described in Experimental Procedures (data not shown), suggesting that residue changes have no gross effects on octameric holoenzyme structure. Electrophoretic resolution of the two subunits is enhanced for enzymes with the histidine tag on IDH1 (Figure 3, lanes 1 and 2) relative to reduced resolution of the subunits for enzymes with the histidine tag on IDH2 (lanes 3 and 4).

Kinetic Analyses of Mutant Enzymes. Kinetic analyses were performed using affinity-purified wild-type and mutant enzymes. $S_{0.5}$ values for isocitrate were measured in the absence or presence of 100 μM AMP, and corresponding Hill coefficients were determined. Apparent V_{max} values were calculated from these kinetic analyses. $S_{0.5}$ values and Hill coefficients for NAD^+ were also measured in the presence

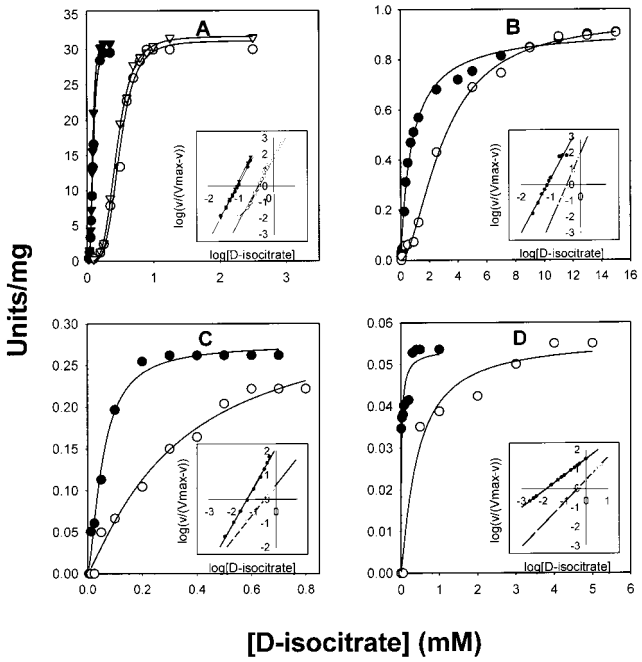

FIGURE 4: Kinetic analyses of wild-type and IDH2 mutant enzymes. Velocity saturation curves for D-isocitrate are shown for assays conducted in the absence (open symbols) or presence (closed symbols) of 100 μM AMP. Data for both wild-type enzymes [IDH1^{His}/IDH2 (circles) and IDH1/IDH2^{His} (triangles)] are shown in panel A. The other panels show data for enzymes with mutant forms of IDH2: IDH1^{His}/IDH2^{R114A} (panel B), IDH1^{His}/IDH2^{Y142F} (panel C), and IDH1^{His}/IDH2^{D248T,D252N} (panel D). Insets show Hill plots of the same data.

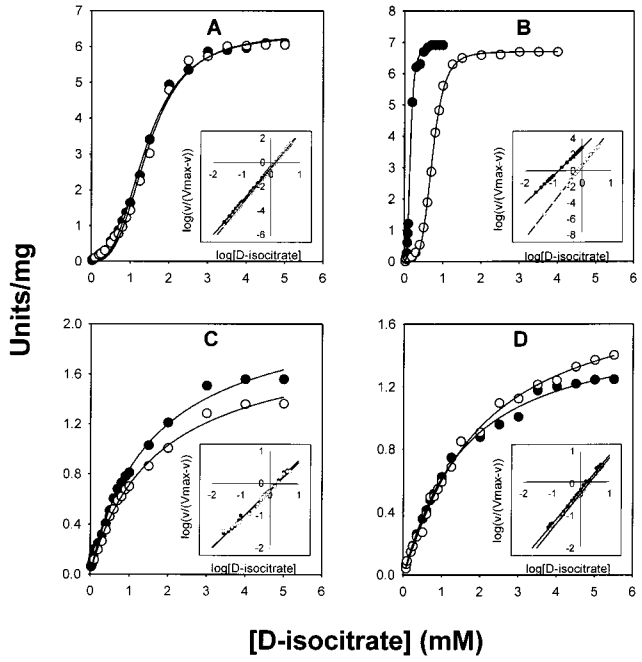

FIGURE 5: Kinetic analyses of IDH1 mutant enzymes. Velocity saturation curves for D-isocitrate are shown for assays conducted in the absence (open symbols) or presence (closed symbols) of 100 μM AMP. The enzymes used in these analyses were IDH1^{A108R}/IDH2^{His} (panel A), IDH1^{F136Y}/IDH2^{His} (panel B), IDH1^{T241D,N245D}/IDH2^{His} (panel C), and IDH1^{A108R,F136Y,T241D,N245D}/IDH2^{His} (panel C). Insets show Hill plots of the same data.

of AMP. Results of kinetic analyses are illustrated in Figures 4 and 5 and summarized in Table 1. As previously reported (*19*, *21*), the two histidine-tagged wild-type enzymes have similar kinetic properties (Figure 4A and Table 1). Apparent V_{max} and $S_{0.5}$ values for isocitrate and NAD^+ are similar. Both enzymes exhibit significant cooperativity with respect to isocitrate (Hill coefficients = 3.5−4.2) and no cooperativity with respect to NAD^+ (Hill coefficients ≅ 1.0). Both enzymes are activated by AMP and exhibit 5.0−5.4-fold reductions in $S_{0.5}$ values for isocitrate in the presence of this allosteric activator. These values are similar to those previously reported for the conventionally purified enzyme (*18*, *30*).

Overall, the residue substitutions in the presumed isocitrate-binding site of IDH2 verify the role of this site in catalysis. The substitution in IDH2 of alanine for Arg-114 (Figure 4B, Table 1), a residue believed to be part of the arginine cluster that forms hydrogen bonds with isocitrate (*17*), produces an ∼30-fold reduction in V_{max} and an ∼6-fold reduction in apparent affinity for isocitrate. Since a similar ∼9-fold increase in $S_{0.5}$ value for isocitrate is also observed in the presence of 100 μM AMP, the IDH2^{R114A} enzyme retains the capacity for allosteric activation. Cooperativity with respect to isocitrate is dramatically reduced for this and other IDH2 mutant enzymes analyzed in this study.

IDH2 mutant enzymes containing Y142F or D248T/D252N substitutions exhibit some significantly different kinetic properties (panels C and D of Figure 4, respectively). V_{max} values are dramatically reduced by ∼100- and ∼300-fold, respectively. Because of these low values, other kinetic parameters shown in parentheses in Table 1 are given as estimates because they cannot be measured with an assurance of accuracy. However, these parameters are sufficient to indicate that both enzymes retain high affinity for isocitrate and the property of allosteric activation by AMP. One interpretation of these results is that Tyr-142 and Asp-248/Asp-252 have crucial roles in catalysis but, unlike Arg-114, may not be essential for high-affinity isocitrate binding. This is consistent with functions of the corresponding Tyr-160 residue of the *E. coli* enzyme, which is important in the dehydrogenation step of the reaction (*29*), and of corresponding Asp-307/Asp-311 residues of the bacterial enzyme, which primarily contribute to binding/coordination of the catalytic divalent cation (*17*). In addition, both IDH2^{Y142F} and IDH2^{D248T,D252N} enzymes exhibit apparent defects in cooperativity with respect to isocitrate. This property is shared with the IDH2^{R114A} enzyme. One interpretation, developed in more detail below, is that modifications within the catalytic site of this enzyme may interfere with communication from the cooperative binding site of IDH1.

As expected, the mutant enzyme containing all four residue changes (R114A, Y142F, D248T, and D252N) in the IDH2 isocitrate-binding site is essentially catalytically inactive, and no kinetic parameters were measurable under standard assay conditions (Table 1). However, because of the implication of roles for Asp-248 and Asp-252 in binding Mg^{2+}, we tested both the IDH2^{D248T,D252N} and IDH2^{R114A,Y142F,D248T,D252N} mutant enzymes in assays with increasing concentrations of $MgCl_2$. This had no effect on kinetic parameters measured for the former enzyme, but for the enzyme containing four residue changes, increasing $MgCl_2$ from the standard 4 mM to apparent saturation at 14 mM produced a velocity of 0.2 unit/mg of enzyme (Table 1), a value ∼150-fold lower than that of wild type. For the IDH2^{R114A,Y142F,D248T,D252N} mutant

Table 1: Kinetic Properties[a] of Mutant Forms of IDH

enzyme	V_{max} (units/mg)	isocitrate $S_{0.5}$ (mM) −AMP/+AMP	isocitrate Hill coeff −AMP/+AMP	NAD^+ $S_{0.5}$ (mM)	NAD^+ Hill coeff
$IDH1^{His}/IDH2$	30.2	0.49/0.09	4.2/3.5	0.21	0.9
$IDH1^{His}/IDH2^{R114A}$	0.9	3.00/0.78	1.8/1.0	0.11	0.8
$IDH1^{His}/IDH2^{Y142F}$	0.3	(0.33/0.06)	(1.2/1.5)	(0.07)	(1.5)
$IDH1^{His}/IDH2^{D248T,D252N}$	0.1	(0.43/0.02)	(1.2/0.8)	(0.06)	(0.6)
$IDH1^{His}/IDH2^{R114A,Y142F,D248T,D252N}$	trace	nd[b]	nd	nd	nd
14 mM Mg^{2+} [c]	*0.2*	*3.64/1.59*	*4.0/2.5*	*0.13*	*1.5*
$IDH1/IDH2^{His}$	31.3	0.45/0.09	3.9/3.7	0.17	1.0
$IDH1^{A108R}/IDH2^{His}$	6.4	1.47/1.41	3.0/2.8	0.65	1.0
2.5 mM NAD^+ [c]	*23.0*	*1.11/1.07*	*2.4/2.4*		
$IDH1^{F136Y}/IDH2^{His}$	6.9	0.73/0.15	4.0/3.5	0.22	1.1
2.0 mM NAD^+ [c]	*23.3*	*0.24/0.09*	*3.9/3.6*		
$IDH1^{T241D,N245D}/IDH2^{His}$	2.2	1.76/1.63	1.0/1.0	2.39	1.0
5 mM NAD^+ [c]	*8.4*	*1.31/1.28*	*1.1/1.2*		
$IDH1^{A108R,F136Y,T241D,N245D}/IDH2^{His}$	1.8	1.49/1.87	1.1/1.1	1.87	1.1
5 mM NAD^+ c	*7.2*	*1.84/1.90*	*1.0/1.0*		

[a] Kinetic analyses were conducted as described in Experimental Procedures. Values were determined from kinetic analyses illustrated in Figures 4 and 5. Assays with varying concentrations of isocitrate were conducted in the absence or presence of 100 μM AMP and, unless otherwise indicated, with 0.5 mM NAD^+ and 4 mM Mg^{2+}. [b] nd = not determined. The minimal catalytic activity of this mutant enzyme precluded measurement of kinetic parameters. [c] Kinetic parameters determined under altered assay conditions are indicated in italics.

enzyme, the $S_{0.5}$ value for isocitrate under these conditions was 3.6 mM, suggesting a significant reduction in affinity. The mutant enzyme exhibits some activation in the presence of AMP, and Hill coefficients calculated in the absence or presence of AMP suggest that the four residue changes do not significantly reduce cooperativity under these assay conditions. Thus, while these results are not directly comparable with those obtained with standard assay conditions, they do indicate that the four residue changes in IDH2 do not completely eliminate catalytic activity. Overall, however, a general conclusion is that individual or collective alterations of these residues in IDH2 have dramatic effects on catalysis, reinforcing the idea that this site in IDH2 is the central site for chemical modification of isocitrate.

Of the residue substitutions made in IDH1, the F136Y replacement produces the fewest effects on kinetic parameters (Figure 5B, Table 1). Other than exhibiting an ~5-fold reduction in apparent V_{max} and modest increases in $S_{0.5}$ values for isocitrate, the $IDH1^{F136Y}$ enzyme appears to retain wild-type characteristics with respect to AMP activation and cooperativity. These results suggest that the phenylalanine residue has a minor function in the putative IDH1 isocitrate-binding site. They also indirectly support the notion that the analogous Tyr-142 residue of IDH2 may contribute little to isocitrate binding per se but may have a primary role in the chemical reaction.

In contrast with F136Y, substitutions of A108R and of T241D/N245D in IDH1 produce distinct changes in kinetic parameters (Figure 5A,C, Table 1). The latter substitutions reduce V_{max} by ~5- and ~14-fold, respectively, relative to the corresponding wild-type enzyme. These are relatively modest decreases in comparison with those produced by complementary residue substitutions in IDH2. Both $IDH1^{A108R}$ and $IDH1^{T241D,N245D}$ enzymes exhibit significant 3−4-fold increases in $S_{0.5}$ values for isocitrate measured in the absence of AMP. These values are unchanged by the presence of AMP, indicating a complete loss of allosteric activation. A possible interpretation of these results, as discussed in more detail in the Discussion section, is that high-affinity binding of isocitrate by IDH1 may be needed for AMP activation. An interesting contrast is the modest effect on cooperativity observed with the A108R substitution in IDH1 as compared to the loss of cooperativity observed with the T241D/N245D substitution. The A108R enzyme is of particular interest because its kinetic properties suggest that cooperativity can be maintained despite a significant reduction in apparent affinity for isocitrate in the IDH1 binding site and a loss of AMP activation.

The mutant enzyme containing all four residue changes in the IDH1 binding site exhibits kinetic characteristics almost identical to those of the $IDH1^{T241D,N245D}$ enzyme; i.e., cooperativity and AMP activation are both absent (Figure 5D, Table 1). Despite these dramatic changes in kinetic parameters, the apparent V_{max} is reduced only ~17-fold for the $IDH1^{A108R,F136Y,T241D,N245D}$ mutant enzyme, consistent with a primary role for IDH1 in regulating rather than directly conducting catalysis.

Kinetic analyses also indicate that residue substitutions in IDH1, with the exception of the F136Y replacement, produce significant effects on apparent affinity for cofactor (Table 1). Therefore, we repeated isocitrate saturation curves for the IDH1 mutant enzymes using higher concentrations of cofactor based on the $S_{0.5}$ values for NAD^+. As shown in Table 1, the increased NAD^+ concentrations have little impact on isocitrate $S_{0.5}$ values and Hill coefficients for the $IDH1^{A108R}$, $IDH1^{T241D,N245D}$, and $IDH1^{A108R,F136Y,T241D,N245D}$ enzymes. However, apparent V_{max} values for these enzymes are dramatically increased to levels 3−4-fold higher than those measured using 0.5 mM NAD^+. A similar increase in measured V_{max} as well as an apparent increase in affinity for isocitrate is observed for the $IDH1^{F136Y}$ enzyme. In contrast to these results for the IDH1 mutant enzymes, increasing NAD^+ concentrations above 0.5 mM produces similar V_{max} values (increases of ≤20%) for the wild-type enzymes and for the IDH2 mutant enzymes (data not shown). This effect on apparent affinity for cofactor for the IDH1 mutant enzymes is considered in more detail below in light of results of previous mutagenesis studies.

We note that some kinetic characteristics are similar to those previously described for mutant enzymes in this study,

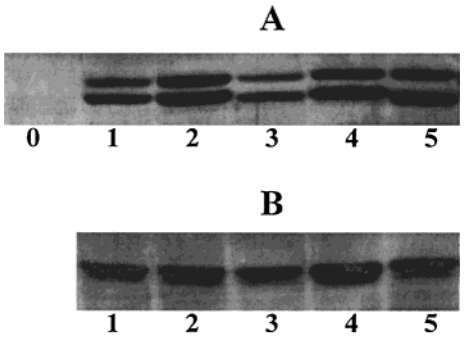

FIGURE 6: Cellular levels of affinity-tagged enzymes. Yeast strains were grown on YP ethanol medium and cells harvested during logarithmic growth. Cellular protein extracts (30 μg each) were electrophoresed and analyzed by immunoblot analysis as described in Experimental Procedures. Panel A shows results for the parental Δ*idh1*Δ*idh2* strain (lane 0) and for transformants of this strain expressing $IDH1^{His}$ with various forms of IDH2 (IDH2, lane 1; $IDH2^{R114A}$, lane 2; $IDH2^{Y142F}$, lane 3; $IDH2^{D248T,D252N}$, lane 4; and $IDH2^{R114A,Y142F,D248T,D252N}$, lane 5). In each lane, the slower migrating band is $IDH1^{His}$. Panel B shows results for transformants expressing $IDH2^{His}$ with various forms of IDH1 (IDH1, lane 1; $IDH1^{A108R}$, lane 2; $IDH1^{F136Y}$, lane 3; $IDH1^{T241D,N245D}$, lane 4; and $IDH1^{A108R,F136Y,T241D,N245D}$, lane 5). In each lane, $IDH2^{His}$ comigrates with IDH1.

e.g., allosteric effects of IDH1 residue substitutions (*23*). However, our changes in assay conditions permit more detailed kinetic analyses as well as measurements of kinetic parameters for IDH2 mutant enzymes previously reported as inactive.

Growth Phenotypes Associated with Expression of Mutant Forms of IDH. The original growth phenotype associated with disruption of *IDH1* and/or *IDH2* genes in yeast is an inability to grow with acetate as a carbon source (*11*). Grivell (*31*) has also reported an increase in the rate of generation of petite segregants in *IDH* gene disruption strains, and we (*32*) have reported that these disruption strains grow poorly with glycerol as a carbon source. We examined these and other growth conditions to determine any correlates among these phenotypes with the wide range of catalytic defects displayed by mutant enzymes in the current study.

Our expression system utilizes centromere-based plasmids that have been shown to produce levels of IDH enzyme expression in an Δ*idh1*Δ*idh2* strain equivalent to those in a parental strain (*19*). In this study, plasmids were transformed into a Δ*idh1*Δ*idh2* yeast strain that exhibits very slow growth with glycerol and permits colorimetric distinction of petite segregants as described in Experimental Procedures. Prior to phenotype analyses, IDH levels in whole cell protein extracts prepared from all transformants were analyzed by immunoblot analysis. As illustrated in Figure 6A, approximately equal levels of the IDH subunits are present in extracts from transformants carrying plasmids encoding $IDH1^{His}$ and authentic or mutant alleles of *IDH2*. Figure 6B shows immunochemical levels of IDH in extracts from transformants carrying plasmids encoding authentic or mutant alleles of *IDH1* with $IDH2^{His}$. In this case, approximately equal amounts of IDH are present in each extract, but due to the histidine tag on IDH2, the two IDH polypeptides comigrate. As we previously reported (*19*), although IDH1 and $IDH2^{His}$ subunits comigrate when electrophoresed in whole cell protein extracts, they can be resolved following purification as shown in Figure 3.

For initial phenotype analyses, transformants expressing wild-type and mutant forms of IDH were streaked onto YP agar plates containing various carbon sources. As shown in Table 2, all of the strains grow well with glucose or ethanol as the carbon source, but the Δ*idh1*Δ*idh2* strain and several strains expressing mutant enzymes fail to grow with acetate as the carbon source. In general, growth on acetate plates appears to correlate with residual IDH activity based on apparent V_{max} values determined for the purified mutant enzymes. Strains expressing IDH2 mutant enzymes that exhibit ≥100-fold decreases in V_{max} values fail to grow on the YP acetate plates. Strains expressing $IDH2^{R114A}$ or any of the IDH1 mutant enzymes do grow on YP acetate plates, although with reduced colony size relative to strains expressing wild-type enzymes.

To obtain more quantitative estimates of growth effects, we measured culture doubling times during logarithmic growth following inoculation into YP glycerol medium as described in Experimental Procedures. As shown in Table 2, transformant strains expressing wild-type IDH grow well under these conditions with doubling times of 2.5 h, whereas the Δ*idh1*Δ*idh2* strain doubles only once over a 30 h period. All transformants expressing IDH1 mutant enzymes grow well under these conditions (doubling times of 3.2−3.7 h), indicating no significant effect on growth due to altered kinetic properties associated with the specific residue replacements. Strains expressing the IDH2 mutant enzymes with reductions of ≥100-fold in V_{max} values have slow doubling times equivalent to that of the disruption strain, indicating the absence of enzyme function in vivo. The strain expressing the $IDH2^{R114A}$ enzyme exhibits an intermediate doubling time of 13 h in this medium. These results suggest that the magnitude of IDH catalytic activity is rate limiting for growth in YP glycerol medium and that alterations in allosteric properties of the enzyme do not significantly affect steady-state growth under this condition.

Finally, we examined the impact of expression of mutant enzymes on the rate of generation of petite segregants. As discussed in more detail below, this respiratory-deficient phenotype for yeast *IDH* disruption mutants was originally attributed to a possible loss of IDH as a mitochondrial mRNA binding protein (*31*). For these assays, transformant strains were cultivated in SC glucose medium to maintain plasmid selection and then plated onto YP glucose to tabulate the relative numbers of petite colonies. As shown in Table 2, ∼4% of the $IDH1^{His}$/*IDH2* and 10% of the *IDH1*/$IDH2^{His}$ transformant colonies are petite, whereas 50% of the colonies from the disruption mutant strain containing an empty plasmid are petite by this test. Similarly, petite frequencies between 46% and 55% were obtained for transformant strains expressing any mutant form of IDH2. These frequencies represent a 12−15-fold increase above that for the strain expressing the parental affinity-tagged enzyme. Among the IDH1 mutant transformants, only the strain expressing the $IDH1^{F136Y}$ enzyme exhibits the same petite frequency as the corresponding wild-type transformant. This is consistent with the relatively mild effects of this residue substitution on kinetic parameters. For the other IDH1 mutant transformants, increases in petite frequency range from 2-fold for the strain expressing the $IDH1^{A108R}$ enzyme to 3.6-fold for the strain expressing the $IDH1^{A108R,F136Y,T241D,N245D}$ enzyme. Thus, there appears to be a relatively good correlation between this

Table 2: Growth Phenotypes of Strains Expressing Mutant Forms of IDH

enzyme expressed	V_{max}[a] (units or fold decrease)	growth on plates (colony size)			culture growth rate[b] (doubling time in h)	% petites[c] (colonies on glucose plates)
		glucose	ethanol	acetate	glycerol	
$IDH1^{His}/IDH2$	30 units/mg	++++	++++	++++	2.5	3.7 (±0.7)
$IDH1/IDH2^{His}$	31 units/mg	++++	++++	++++	2.5	10.0 (±2.4)
none[d]		++++	++++	−	30.0	49.5 (±8.8)
$IDH1^{His}/IDH2^{R114A}$	↓30×	+++	+++	++	13.0	45.7 (±9.9)
$IDH1^{His}/IDH2^{Y142A}$	↓100×	+++	+++	−	28.0	54.7 (±10.3)
$IDH1^{His}/IDH2^{D248T,D252N}$	↓300×	+++	+++	−	27.0	52.3 (±5.0)
$IDH1^{His}/IDH2^{R114A,Y142F,D248T,D252N}$	↓>300×	+++	+++	−	28.5	50.3 (±10.2)
$IDH1^{A108R}/IDH2^{His}$	↓5×	++++	++++	++	3.3	19.9 (±2.6)
$IDH1^{F136Y}/IDH2^{His}$	↓5×	++++	++++	+++	3.2	10.8 (±2.3)
$IDH1^{T241D,N245D}/IDH2^{His}$	↓14×	++++	++++	++	3.7	31.7 (±0.2)
$IDH1^{A108R,F136Y,T241D,N245D}/IDH2^{His}$	↓17×	++++	+++	++	3.7	36.1 (±6.3)

[a] Values are based on those in Table 1. [b] Values are averages of two independent experimental determinations. [c] Values are from three independent determinations. [d] The Δ*idh1*Δ*idh2* strain was used for plate and culture growth assays conducted with rich YP medium. For analysis of petite frequencies, which requires precultivation on minimal medium, the disruption strain was transformed with the pRS316 plasmid lacking *IDH* genes.

Table 3: Summary of Kinetic Effects[a] of Residue Substitutions in IDH Active Sites

IDH2 active site						IDH1 active site					
		$S_{0.5}$		cooperativity	AMP			$S_{0.5}$		cooperativity	AMP
substitution	V_{max}	isocitrate	NAD^+	(isocitrate)	activation	substitution	V_{max}	isocitrate	NAD^+	(isocitrate)	activation
R114A	↓30×	6×	<1×	−	+	A108R	↓5×	4×	4×	+	−
Y142F	↓100×	1×	<1×	−	+	F136Y	↓5×	2×	1×	+	+
D248T, D252N	↓300×	1×	<1×	−	+	T241D, N245D	↓14×	4×	10×	−	−
R114A, Y142F, D248T, D252N	↓>300×	nd	nd	nd	nd	A108R, F136Y, T241D, N245D	↓17×	3×	10×	−	−
S98A[b]	↓160×	3×	6×	+	+	S92A[b]	↓14×	3×	20×	−	−
K183′A[c]	NA[d]	nd	nd	nd	nd	K189′A[c]	↓2×	1×	3×	−	−
D217′A[c]	NA	nd	nd	nd	nd	D222′A[c]	↓18×	1×	6×	−	−

[a] Magnitude of changes in kinetic parameters relative to corresponding histidine-tagged wild-type enzymes. [b] Kinetic analyses of these enzymes were previously reported for partially purified enzymes (*18*). Values reported here were determined with affinity-purified enzymes. [c] Kinetic analyses were previously reported (*21*). [d] NA = no activity; nd = not determined.

phenotype and effects on V_{max} values. However, the 2-fold difference in petite frequencies observed for strains expressing $IDH1^{A108R}$ and $IDH1^{F136Y}$ enzymes suggests that further refinement may allow distinction among mutant enzymes that exhibit similar reductions in V_{max} but differences in other kinetic parameters.

DISCUSSION

Because NAD^+-specific isocitrate dehydrogenase is believed to play a central role in allosteric control of aerobic energy production, the physical and kinetic properties of the yeast enzyme were analyzed in great detail years ago by Atkinson and colleagues (*30*, *33*, *34*). They reported that the purified enzyme contained eight apparently identical subunits on the basis of sedimentation experiments and electrophoresis (*33*). However, their ligand-binding studies, which demonstrated twice as many isocitrate as NAD^+ or divalent cation-binding sites, led them to propose a nonequivalence of function for component subunits (*34*). Subsequent physical and genetic analyses (*10*−*13*) have indicated that the octameric enzyme is composed of four each of two similar but nonidentical subunits. Sequence analysis and the current study contribute evidence for distinct sites within each type of subunit that cooperatively bind isocitrate (IDH1) or catalytically bind isocitrate/Mg^{2+} (IDH2). In this study, the residue changes chosen to examine the putative active sites of IDH1 and IDH2 were based on four specific differences in models derived from the known three-dimensional structure for *E. coli* isocitrate dehydrogenase. Kinetic analyses of resulting mutant enzymes are summarized in Table 3, along with results of previous mutagenesis studies of other residues in the active sites (*18*, *21*).

One obvious general conclusion is that alterations within the IDH2 active site have far more dramatic effects on catalysis than do analogous substitutions in IDH1, consistent with the catalytic function implied by a one-to-one correspondence of IDH2 residues in this site with those of the bacterial enzyme (Figure 1). Results of specific residue replacements in IDH2 correlate well with assigned functions for analogous residues in the *E. coli* enzyme. IDH2 Ser-98, as mentioned above, appears to correlate with bacterial Ser-113, a residue important for binding isocitrate and the target for regulation in bacterial cells by phosphorylation/inactivation (*4*, *5*). In this study, the Y142F replacement in IDH2 was found to produce results very similar to those of a Y160F replacement in the bacterial enzyme, i.e., a dramatic decrease in the rate of catalysis but little effect on the K_m for isocitrate (*29*). These and other results (*35*) led to the conclusion that this tyrosine residue in the bacterial enzyme is important in the dehydrogenation step of the reaction. Similarly, bacterial Lys-230′ was determined to be essential for the decarboxylation step of the reaction (*29*, *35*), and we previously found that an alanine replacement for the analogous Lys-183′ residue results in a catalytically inactive enzyme (*21*). Lys-183′ and Asp-217′ (the analogue of bacterial Asp-283′) are IDH1 residues believed to contribute to the catalytic active

site of IDH2. Finally, IDH2 Asp-248 and Asp-252 appear to be analogues of bacterial Asp-307 and Asp-311, residues that, based on crystallographic structure, are important for binding the essential divalent cation. We find that replacement of these two aspartate residues produces a yeast enzyme that exhibits very little catalytic activity but that retains significant affinity for isocitrate, consistent with a specific role in binding Mg^{2+}. Since elevated Mg^{2+} concentrations do not improve activity of the $IDH2^{D248T,D252N}$ enzyme but do improve activity of the $IDH2^{R114A,Y142F,D248T,D252N}$ enzyme, direct ligand-binding analyses will be necessary to distinguish roles of these residues.

With respect to isocitrate $S_{0.5}$ values for the yeast mutant enzymes (Table 3), it should be noted that these values may significantly underestimate effects on isocitrate binding at sites in either mutant subunit, since the other subunit site may retain high affinity. Kuehn et al. (*34*) reported that all isocitrate-binding sites in the yeast enzyme have similar affinities. Thus, an overall 2-fold increase in $S_{0.5}$ relative to the wild-type value could be indicative of significant changes within one altered subunit. Among IDH2 mutant enzymes with sufficient residual catalytic activity to obtain reliable estimates for $S_{0.5}$ values, both the R114A and S98A enzymes exhibit significant reductions in apparent affinity for isocitrate. These results suggest that Arg-114 and Ser-98 are critical residues for substrate binding. Residue replacements in the putative isocitrate-binding site of IDH1 have much more moderate effects on catalysis, but many significantly reduce the apparent affinity for isocitrate (Table 3). These results support the idea that the "active" site of IDH1 binds but does not catalytically alter isocitrate. The two IDH1 active site substitutions that produce no effect on isocitrate $S_{0.5}$ are those for Lys-189′ and Asp-222′ (*21*). Since these residues are donated by IDH2, they may be more important for communication between the active sites than in isocitrate binding per se.

With respect to allosteric properties of the enzyme, we propose that binding of isocitrate by the IDH1 site is important for cooperativity. This is supported by the loss of cooperativity for most of the mutant enzymes with residue replacements in the putative IDH1 site (Table 1). However, defects in cooperativity are also observed for several mutant enzymes with residue substitutions in IDH2. This could mean that both active sites participate in cooperative binding of isocitrate. Alternatively, IDH1 may be the primary cooperative binding site, but defects in IDH2 may prevent appropriate kinetic response; i.e., they may interfere with transmission of information from the IDH1 binding site.

More clear is the correlation between the IDH1 isocitrate-binding site and AMP activation, since most alterations within this site result in loss of positive activation (Table 3). In contrast, AMP activation is retained in all IDH2 mutant enzymes with sufficient residual activity for kinetic analysis. This suggests that the site in IDH1 is essential for allosteric activation. These results correlate well with results of ligand-binding studies performed by Kuehn et al. (*34*). Those investigators demonstrated that the presence of isocitrate was essential to obtain binding of AMP and suggested, as our results imply, that binding of isocitrate at noncatalytic sites of the enzyme is an essential prerequisite for binding and allosteric activation by AMP. Also, although we cannot rule out a direct overlap between AMP and IDH1 isocitrate-binding sites, we previously described a mutant enzyme with targeted substitutions in the presumed AMP-binding site in IDH1 (*19*). This enzyme demonstrated a loss of AMP activation with little effect on cooperativity, suggesting that the AMP-binding site is distinct from the IDH1 isocitrate-binding site.

Another clear correlation is the detrimental effect of residue replacements in IDH1 on the $S_{0.5}$ value for NAD^+ (Table 3). In contrast, replacements in IDH2 generally do not affect this kinetic parameter. The $IDH2^{S98A}$ enzyme is an exception, as discussed below. The increases of 3−20-fold in NAD^+ $S_{0.5}$ values associated with IDH1 residue replacements are significant but substantially less than the 80-fold increase in the $S_{0.5}$ value previously measured for a mutant enzyme with specific residue replacements in the putative NAD^+-binding site in IDH2 (*19*). Thus, it seems likely that these IDH1 effects on apparent affinity for NAD^+ are indirect. Since Kuehn et al. (*34*) found that NAD^+ binding to the yeast enzyme was measurable only in the presence of isocitrate, it seems possible that binding of isocitrate to IDH1 enhances binding of cofactor as well as of AMP, as described above. This idea is supported by the dramatic increases in V_{max} values for the IDH1 mutant enzymes obtained when assay levels of NAD^+ are increased (Table 1).

We believe that the ∼6-fold increase in the $S_{0.5}$ value for NAD^+ observed for the $IDH2^{S98A}$ enzyme is also informative in light of functions assigned for the analogous Ser-113 residue of the bacterial enzyme. The side chain of Ser-113 forms a hydrogen bond with the γ-carboxylate of bound isocitrate, and a salt bridge between the γ-carboxylate and the nicotinamide ring stabilizes the nicotinamide mononucleotide moiety of $NADP^+$, which makes few other contacts with the enzyme (*17*, *35*). As a consequence, substitutions of various residues for Ser-113 have different detrimental effects on the K_m value for isocitrate, but all increase the K_m for $NADP^+$ by ∼10-fold (*36*). The similar increase in $S_{0.5}$ for NAD^+ observed for the S98A substitution suggests a similar catalytic function for this IDH2 residue.

At this point, our speculations about effects of residue substitutions on binding of substrate, cofactor, or allosteric modifier are based solely on kinetics and will be further explored by direct binding assays. Preliminary analyses indicate that the mutant enzymes from this study containing all four residue changes in IDH1 or in IDH2 retain the same number of isocitrate-binding sites as the wild-type enzyme.[2] Thus, while these residue changes clearly affect subunit function, they appear to be permissive for isocitrate binding as we had predicted. Also, although these kinetic analyses have clarified our understanding of distinct and interdependent functions of the IDH1 and IDH2 subunits, some key aspects of structure and function remain unexplained. For example, our simple assumptions about essentially independent binding sites in each subunit would lead to a conclusion that each octameric enzyme would be capable of binding eight molecules of isocitrate and four each of Mg^{2+} (by IDH2), NAD^+ (by IDH2), and AMP (by IDH1). However, ligand-binding studies (*34*) indicate that there are, per octamer, four isocitrate-binding sites and only two sites for binding NAD^+, Mg^{2+}, and AMP. Thus, deciphering the

[2] A-P. Lin and L. McAlister-Henn, unpublished results.

interactions and arrangements of subunits in the holoenzyme is of significant interest and will require focused structural analyses.

In addition to probing differential functions of its homologous subunits, we are interested in using mutant forms of IDH with well-defined kinetic defects to dissect key functions of the enzyme in vivo. Therefore, transformants expressing the mutant enzymes constructed in this study were analyzed for growth phenotypes previously attributed to yeast mutants containing *IDH1* and/or *IDH2* gene disruptions including an inability to grow with acetate as a carbon source (*11*), slow growth with glycerol (*32*), and an increase in petite segregants (*31*). A general conclusion is that phenotypes similar to those of disruption mutant strains are obtained with expression of mutant forms of IDH exhibiting $\geq\sim$100-fold decreases in V_{max} values. Thus, these phenotypes can result from loss of IDH catalytic function as well as from loss of IDH polypeptides.

The inability to grow with acetate as a carbon source is a phenotype exhibited by several other yeast tricarboxylic acid cycle mutants (*13*, *14*, *22*), suggesting a direct correlation with enzymatic dysfunction in this pathway in vivo. The slow glycerol growth phenotype was previously observed for several tricarboxylic acid cycle mutants including IDH null or nonsense mutants but not for an IDH2^{R104K} missense mutant, suggesting that the phenotype was due to the physical absence of holoenzyme (*32*). However, the clear correlation between IDH activity and glycerol growth reported here suggests that the slow glycerol growth phenotype can result from catalytic dysfunction as well as the physical absence of the protein. Thus, one possibility is that the mutant IDH2^{R104K} enzyme may retain sufficient residual activity in vivo for growth on glycerol due to a relatively conservative substitution in an active site residue. Our reason for interest in this point is an additional aspect of the glycerol growth phenotype apparently unique to IDH null and nonsense mutants. Growth of these mutants on glycerol can be enhanced by secondary mutations affecting citrate synthase and other tricarboxylic acid cycle and oxidative functions (*22*, *32*). This suppression was interpreted to imply metabolic and/or structural interactions among these enzymes. It will therefore be of interest to determine if the glycerol growth phenotypes of mutants with well-defined catalytic lesions in IDH can also be suppressed by the mutations affecting other oxidative enzymes.

The basis for the increase in petite frequency associated with reduced IDH activity is unclear. Grivell (*31*) suggested that an increase in petite frequency associated with *IDH* gene disruption mutants may be due to detrimental effects on mitochondrial translation. This idea was based on the observation that IDH can bind to specific regions within the 5′-untranslated regions of all yeast mitochondrial mRNAs (*7*, *37*). De Jong et al. (*8*) have also recently shown that the absence of IDH results in a 2−3-fold increase in mitochondrial translation, suggesting that the binding of IDH normally inhibits translation in vivo. In addition, we have found that RNA transcripts containing IDH binding sequences can dramatically and allosterically inhibit IDH activity in in vitro assays (*9*), suggesting a possible reciprocal mechanism for control of translation and tricarboxylic acid cycle flux. Collectively, these observations, and the fact that respiratory deficiency is a common phenotype associated with defects in mitochondrial translation in yeast (*38*), suggest a basis for the increased petite frequency of *IDH* gene disruption mutants. However, our finding that petite frequency is substantially elevated in transformants expressing IDH mutant enzymes suggests that catalytic defects can also produce this phenotype and/or that residue replacements in these enzymes may affect association with mitochondrial mRNAs. Tests to distinguish between these possibilities are in progress.

ACKNOWLEDGMENT

We thank Dr. Karyl I. Minard for technical advice and HPLC analyses, Sondra L. Anderson for technical support, Luis Brieba for assistance in mutagenesis, and Dr. Kosaku Uyeda for providing isocitrate.

REFERENCES

1. Chen, R. F., and Plaut, G. W. E. (1963) *Biochemistry 2*, 1023−1032.
2. Hathaway, J. A., and Atkinson, D. E. (1963) *J. Biol. Chem. 238*, 2875−2881.
3. Garnak, M., and Reeves, H. C. (1979) *Science 203*, 1111−1112.
4. Thorsness, P. E., and Koshland, D. E., Jr. (1987) *J. Biol. Chem. 262*, 10422−10425.
5. Dean, A. M., Lee, M. H. I., and Koshland, D. E., Jr. (1989) *J. Biol. Chem. 264*, 20482−20486.
6. LaPorte, D. C., Walsh, K., and Koshland, D. E., Jr. (1984) *J. Biol. Chem. 259*, 10468−14075.
7. Elzinga, S. D. J., Bednarz, A. I., van Oosterum, K., and Grivell, L. A. (1992) *Nucleic Acids Res. 21*, 5328−5331.
8. De Jong, L., Elzinga, S. D. J., McCammon, M. T., Grivell, L. A., and van der Spek, H. (2000) *FEBS Lett. 24194*, 1−5.
9. Anderson, S. L., Minard, K. I., and McAlister-Henn, L. (2000) *Biochemistry 39*, 5623−5629.
10. Keys, D. A., and McAlister-Henn, L. (1990) *J. Bacteriol. 172*, 4280−4287.
11. Cupp, J. R., and McAlister-Henn, L. (1991) *J. Biol. Chem. 266*, 22199−22205.
12. Cupp, J. R., and McAlister-Henn, L. (1992) *J. Biol. Chem. 267*, 16417−16423.
13. McAlister-Henn, L., and Thompson, L. M. (1987) *J. Bacteriol. 169*, 5157−5166.
14. Kim, K., Rosenkrantz, M. S., and Guarente, L. (1986) *Mol. Cell. Biol. 6*, 1936−1942.
15. Hurley, J. H., Dean, A. M., Thorsness, P. E., Koshland, D. E., Jr., and Stroud, R. M. (1990) *Proc. Natl. Acad. Sci. U.S.A. 86*, 8635−8639.
16. Hurley, J. H., Dean, A. M., Thorsness, P. E., Koshland, D. E., Jr., and Stroud, R. M. (1990) *J. Biol. Chem. 265*, 3599−3602.
17. Hurley, J. H., Dean, A. M., Koshland, D. E., Jr., and Stroud, R. M. (1991) *Biochemistry 30*, 8671−8678.
18. Cupp, J. R., and McAlister-Henn (1993) *Biochemistry 32*, 9323−9328.
19. Zhao, W.-N., and McAlister-Henn, L. (1997) *J. Biol. Chem. 272*, 21811−21877.
20. Hurley, J. H., Chen, R., and Dean, A. M. (1996) *Biochemistry 35*, 5670−5678.
21. Panisko, E. A., and McAlister-Henn, L. (2001) *J. Biol. Chem. 276*, 1204−1210.
22. Przybyla-Zawislak, B., Gadde, D. M., Ducharme, K., and McCammon, M. T. (1999) *Genetics 152*, 153−166.
23. Panisko, E. A. (2000) Ph.D. Dissertation, University of Texas Health Science Center, San Antonio.
24. Sikorski, R. S., and Hieter, P. (1989) *Genetics 122*, 19−27.
25. Bradford, M. M. (1976) *Anal. Biochem. 72*, 248−254.

26. Haselbeck, R. J., and McAlister-Henn, L. (1993) *J. Biol. Chem. 268*, 12116−12122.
27. Pace, C. N., Vajdos, F., Fee, L., Grimsley, G., and Gray, T. (1995) *Protein Sci. 4*, 2411−2423.
28. Hanes, C. S. (1932) *Biochem. J. 26*, 1406−1421.
29. Lee, M. E., Dyer, D. H., Klein, O. D., Bolduc, J. M., Stoddard, B. L., and Koshland, D. E., Jr. (1995) *Biochemistry 34*, 378−384.
30. Barnes, L. D., McGuire, J. J., and Atkinson, D. E. (1972) *Biochemistry 11*, 4322−4328.
31. Grivell, L. A. (1995) *Crit. Rev. Biochem. Mol. Biol. 30*, 121−164.
32. Gadde, D. M., and McCammon, M. T. (1997) *Arch. Biochem. Biophys. 344*, 139−149.
33. Barnes, L. D., Kuehn, G. D., and Atkinson, D. E. (1971) *Biochemistry 10*, 3939−3944.
34. Kuehn, G. D., Barnes, L. D., and Atkinson, D. E. (1971) *Biochemistry 10*, 3945−3951.
35. Bolduc, J. M., Dyer, D. H., Scott, W. G., Singer, P., Sweet, R. M., Koshland, D. E., Jr., and Stoddard, B. L. (1995) *Science 268*, 1312−1318.
36. Dean, A. M., Shiau, A. K., and Koshland, D. E., Jr. (1996) *Protein Sci. 5*, 341−347.
37. Dekker, P. J. T., Stuurman, J., van Oosterum, K., and Grivell, L. A. (1992) *Nucleic Acids Res. 21*, 5328−5331.
38. Myers, A. M., Pape, L. K., and Tzagoloff, A. (1985) *EMBO J. 4*, 2087−2092.
39. Rost, B. (1995) in *The Third International Conference on Intelligent Systems for Molecular Biology* (ISMB) (Rawlings, C., Clark, D., Altman, R., Hunter, L., Lengauer, T., and Wodak, S., Eds.) pp 314−321, AAAI Press, Cambridge, England.
40. Rice, D. W., and Eisenberg (1997) *J. Mol. Biol. 267*, 1026−1038.

BI0111707